

## Coherent coupling dynamics in a quantum-dot microdisk laser

D. K. Young, L. Zhang, D. D. Awschalom, and E. L. Hu

Center for Spintronics and Quantum Computation, University of California, Santa Barbara, California 93106

(Received 23 April 2002; published 29 August 2002)

Luminescence intensity autocorrelation (LIA) is employed to investigate coupling dynamics between (In, Ga)As quantum dots (QD's) and a high- $Q$  ( $\sim 7000$ ) resonator with ultrafast time resolution (150 fs), below and above the lasing threshold at  $T=5$  K. For QD's resonant and nonresonant with the cavity we observe both a sixfold enhancement and a 0.77-time reduction of the spontaneous emission rate, respectively. In addition, LIA spectroscopy reveals the onset of *coherent* coupling at the lasing threshold through qualitative changes in the dynamic behavior and a tripling of the resonant QD emission rate.

DOI: 10.1103/PhysRevB.66.081307

PACS number(s): 03.67.Lx, 42.55.Sa, 78.47.+p, 78.67.-n

The ability to control spontaneous emission<sup>1</sup> in the solid state is expected to improve laser devices<sup>2</sup> as well as enable the development of systems for quantum cryptography, such as single-photon sources.<sup>3</sup> "Self-assembled" InAs quantum dots (QD's) integrated within high- $Q$  microcavities provide an ideal test bed for studying the control of QD emission through cavity QED (Purcell effect).<sup>4,5</sup> Moreover, understanding the coupling dynamics between the QD's and microcavity may provide an avenue for performing quantum computation and communication with electron spins.<sup>6</sup> Previous measurements in microcavities (i.e., micropillars,<sup>4</sup> microdisks,<sup>5</sup> and microspheres<sup>7</sup>) have explored enhanced spontaneous QD emission (relative to the unprocessed material), and have yet to investigate the coupling dynamics near the onset of lasing.

Here we report time-resolved measurements in microdisks with integrated QD's below and above the lasing threshold using luminescence intensity autocorrelation (LIA) spectroscopy,<sup>8</sup> where the time resolution is theoretically limited by the optical pump/probe pulse widths ( $\sim 150$  fs). Detailed studies of the QD-cavity coupling dynamics have shown for QD's resonant and nonresonant with the cavity a sixfold enhancement and a 0.77-time reduction of the spontaneous emission rate, respectively. Moreover, we use LIA spectroscopy to measure the onset of *coherent coupling* between the QD's and cavity at the lasing threshold, where we observe a clear signature at zero time delay between pump and probe pulses and an additional tripling of the resonant QD emission rate due to stimulated emission.

The device structure is grown by molecular-beam epitaxy upon a semi-insulating GaAs substrate with an AlAs/GaAs buffer. A 1- $\mu\text{m}$  layer of  $\text{Al}_x\text{Ga}_{1-x}\text{As}$  ( $x$  ranging from 0.65–0.85) is subsequently grown, determining the microdisk post height. The disk region has a single layer of (In, Ga)As self-assembled QD's with a dot density of  $10^9\text{ cm}^{-2}$  and is clad symmetrically by 100-nm GaAs, 20-nm  $\text{Al}_{0.3}\text{Ga}_{0.7}\text{As}$ , and 4-nm GaAs [right inset of Fig. 1(a)]. The microdisks have  $\sim 4\text{-}\mu\text{m}$  diameters defined by photolithography, yielding an effective modal volume  $V \sim 10(\lambda/n)^3$  [assuming the dominating modes are guided primarily around the circumference of the microdisk,<sup>9</sup> i.e., whispering gallery modes (WGM's)], where  $n$  is the effective refractive index of the cavity and  $\lambda$  is the emission wavelength. WGM's arise due to total internal reflection, relying on the large index contrast between the

semiconductor/air interface, where light is reflected along the curved inner boundary of the cavity.<sup>10</sup> Details of the two-step wet etch process and stimulated emission from QD's integrated in microdisks can be found elsewhere.<sup>9</sup> In order to minimize thermal broadening of the QD emission, all data is taken at  $T=5$  K in a liquid-helium-flow optical cryostat and is collected from the side of the disk to maximize the collection efficiency of the WGM emission. Time-integrated pho-

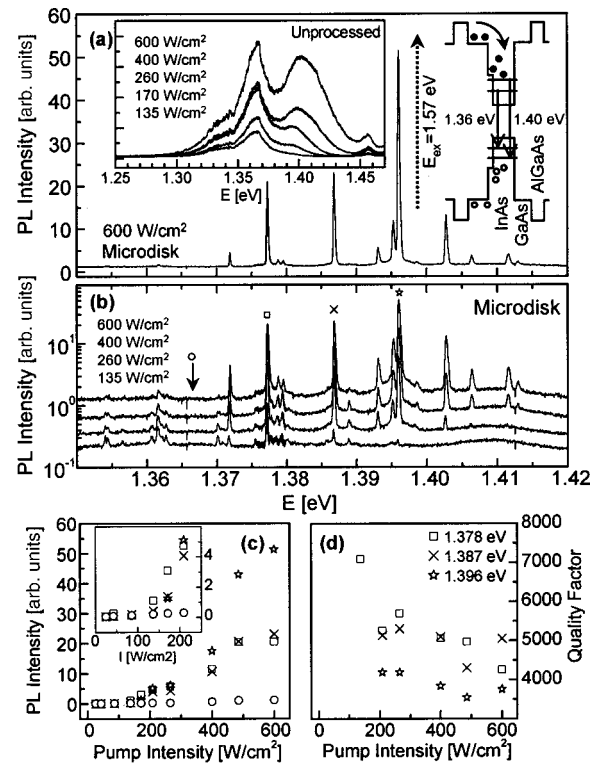


FIG. 1. Time-integrated photoluminescence (PL) characteristics. (a) Multimode lasing from a high- $Q$  microdisk integrated with QD's. Intensity-dependent QD PL from unprocessed material (left inset). Band diagram showing excitation into GaAs and subsequent relaxation into QD ground and excited states (right inset). (b) Intensity-dependent PL from the microdisk. (c) Nonlinear PL intensity dependence for three whispering gallery modes (WGM's). Symbols defined in (b). QD's nonresonant with the cavity show linear dependence. Expanded view (inset). (d) WGM quality factors  $Q$  measured at intensities above their lasing thresholds.

toluminescence (PL) is spectrally analyzed with a 0.5-m spectrometer coupled to a  $LN_2$  cooled charge coupled detector yielding resolution of 50  $\mu\text{eV}$ .

The PL data taken on unprocessed (i.e., as-grown) QD material [Fig. 1(a), left inset] shows the characteristic broad spectrum at various pump intensities denoting the variation in size (13%) of the QD's. Increasing excitation intensity gives rise to increased emission at higher energies, suggesting occupation of, and subsequent emission from, higher-energy QD transitions. Nonresonant excitation ( $E_{\text{ex}} = 1.57 \text{ eV}$ ) into the GaAs layer is used to increase carrier generation due to the small absorption cross section of the QD's.<sup>9</sup> Subsequent relaxation into the QD's occurs on very short time scales (carrier capture time  $\sim 20 \text{ ps}$ ).<sup>5</sup> Figure 1(b) shows multimode lasing under similar conditions of QD's within a microdisk (note semilog scale). Indeed, PL from the microdisk is shown above lasing threshold on a linear scale [Fig. 1(a)]. Quality factors,  $Q$ , as high as 7000 are determined by computing  $Q = E/\Delta E$ , where  $\Delta E$  is the full width at half maximum of the emission energy. The enhancement of the spontaneous emission rate is given by the Purcell factor,<sup>1</sup>  $F_P$  (which indicates the degree of coupling between emitter and cavity):  $F_P = (3/4\pi^2)(Q\lambda^3/V)$ . For our highest- $Q$  WGM, with transition energy at 1.378 eV, we estimate  $F_P \sim 50$ . This calculation assumes an *ideal* monochromatic emitter that is spatially and spectrally coupled to the mode, however, due to nonidealities in coupling between emitter and cavity as well as cavity mode degeneracy,<sup>5</sup> we expect the actual  $F_P$  measured through the spontaneous emission lifetime to be smaller.

We employ luminescence intensity autocorrelation,<sup>8</sup> a time-resolved technique that measures the nonlinear dependence of PL with excitation intensity to obtain the radiative lifetime of the QD excitonic states. LIA data are obtained using two energetically degenerate 150-fs pulses from a Ti-sapphire laser where relative time delay is controlled by a mechanical delay line. Optical choppers modulate the two equally intense excitation beams at different frequencies while phase-sensitive detection at the sum frequency measures nonlinear changes in PL intensity that arise from the temporal overlap of the carrier populations excited by the two pulses. The normal-incident excitation is focused to a spot ( $\sim 30 \mu\text{m}$ ) that is much larger than the microdisk diameter, ensuring uniform excitation of the cavity. PL in the time-resolved data is spectrally analyzed with a high throughput spectrometer with spectral resolution ( $\sim 5 \text{ meV}$ ) and detected with an InGaAs photodiode.

Each point in the LIA scan is the *time-integrated* nonlinear PL response for a given time delay between the two excitation beams. Moreover, there are two major contributions to the signal: (a) differential absorption and (b) "cross recombination." Differential absorption arises due to state filling (i.e., the excitation from the first beam makes the second beam less likely to excite as many carriers, due to fewer available states), resulting in a negative LIA signal. In cross recombination, electrons/holes from one pulse recombine with holes/electrons from the other, and result in a positive LIA signal. In our measurements, the PL intensity from one pulse increases in the presence of the second pulse, indicat-

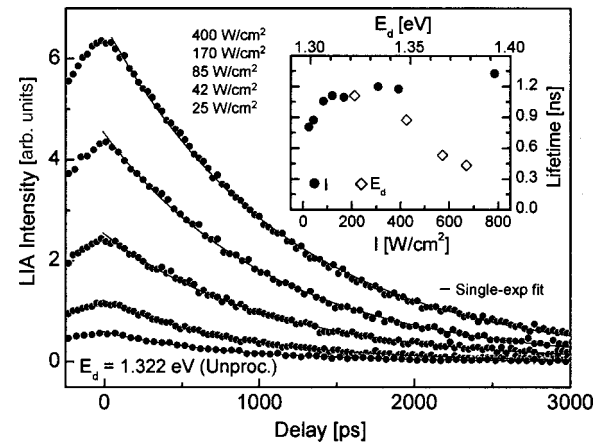


FIG. 2. Time-resolved QD PL characteristics in unprocessed material. Intensity-dependent luminescence intensity autocorrelation (LIA) data detected at QD energy ( $E_d = 1.322 \text{ eV}$ ). Lifetimes extracted from decaying single-exponential fits (solid lines) are plotted as a function of pump intensity (filled circles) for fixed  $E_d$ , and  $E_d$  (diamonds) for fixed pump intensity ( $300 \text{ W cm}^{-2}$ ) (inset).

ing that the LIA is determined by the radiative cross recombination of the excitons and provides a measure of their lifetimes.

To compare emission rates, we measured the intrinsic lifetimes of QD's in an unprocessed part of the sample. Figure 2 shows the intensity dependence of LIA data taken at a detection energy  $E_d = 1.322 \text{ eV}$ , a ground-state energy within the QD ensemble. LIA data are fit to a single-exponential  $A \exp(-t/\tau)$  to extract the decay time of the recombining excitons. Since the beams are equal in intensity,<sup>11</sup> LIA data is expected to be symmetric around  $t=0$ , as is observed. The data is well fit by a single exponential, yielding lifetimes that agree with conventional time-resolved PL measurements.<sup>12</sup> For all extracted lifetimes, the error is smaller than the plotted symbol size or otherwise noted by error bars. QD spontaneous emission rates have been observed to decrease with increasing QD size,<sup>12</sup> despite theoretical predictions that the QD oscillator strength should remain nearly independent of QD size.<sup>13</sup> We observe similar behavior in the LIA lifetimes of our unprocessed control samples (Fig. 2, inset), whose insensitivity to pump intensity suggests that they measure the QD spontaneous emission rate.

In contrast, the data from processed microdisk samples show completely different behavior due to the presence of WGM's. The intensity dependence of the time-integrated PL from QD's within the microdisks is shown in Fig. 1(c). Transitions coupled to the WGM's show nonlinear dependence of PL intensity on excitation intensity, revealing lasing thresholds ( $I_{\text{TH}} \sim 150\text{--}200 \text{ W cm}^{-2}$ ). In contrast, for QD's off resonant with a cavity mode (circles;  $E_d = 1.366 \text{ eV}$ ), there is a linear dependence on pump intensity (shown also in an expanded view in the inset). In addition, at lasing threshold, the quality factor  $Q$  is largest and monotonically decreases with higher pump intensity [Fig. 1(d)], while below threshold,  $Q \sim 1$ . Similar broadening in quantum well microdisk cavities at intensities above lasing threshold<sup>14</sup> is typically associated with free-carrier absorption (FCA), however, QD

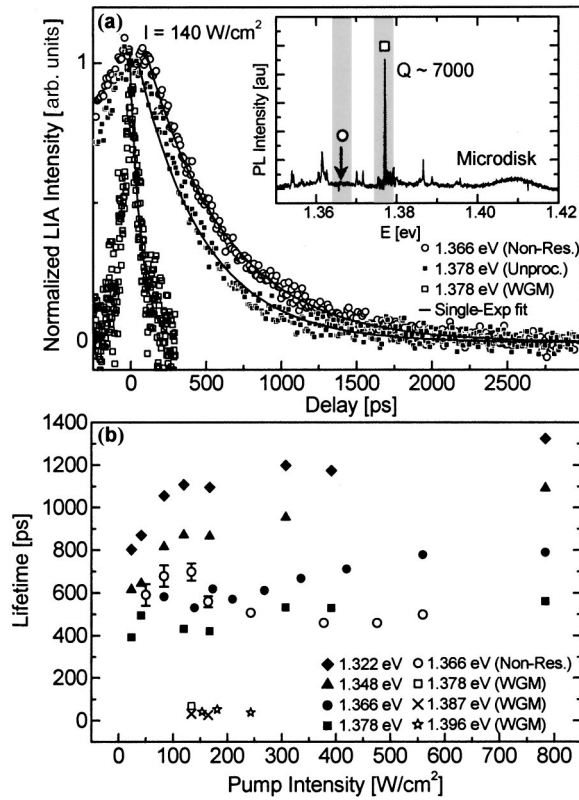


FIG. 3. (a) Sixfold enhancement in the spontaneous emission rate is observed when comparing normalized LIA data between QD's resonant with a WGM (squares) to energetically degenerate (ED) QD's in unprocessed material (filled squares). QD's nonresonant with a WGM (circles) under same conditions indicate enhancement is indeed due to Purcell effect. PL taken under same conditions (inset). Shaded regions represent spectral resolution in time-resolved measurements. (b) Summary of below threshold lifetimes for QD's outside the cavity (filled symbols), as well as QD's resonant and nonresonant with a WGM (unfilled symbols). Below lasing threshold of a nearby mode, inhibited spontaneous emission is observed when comparing QD's nonresonant (circles) within the cavity to the ED QD's (filled circles) outside the cavity.

emitters in microdisk cavities with continuous-wave excitation do not suffer from FCA at lasing threshold.<sup>9</sup> The decrease in  $Q$  may reflect the increased number of QD's becoming resonant with the cavity mode at higher intensities, as well as emission broadening from shorter lifetimes, or increased carrier densities with pulsed excitation.<sup>15</sup>

In Fig. 3(a), normalized LIA data from QD's resonant (squares) and nonresonant (circles) with a WGM ( $Q \sim 7000$ ), as well as energetically degenerate (ED) QD's (filled squares) in an unprocessed part of the sample are compared for a given intensity ( $I = 140 \text{ W cm}^{-2}$ ) near lasing threshold of  $E = 1.378 \text{ eV}$ . PL from the microdisk under the same conditions is shown (inset). There is a large reduction in the spontaneous emission lifetime from QD's that are resonant with the WGM (squares;  $\tau = 70 \text{ ps}$ ) when compared to both ED QD's outside the cavity (filled squares;  $\tau = 430 \text{ ps}$ ) and nonresonant QD's in the cavity (circles;  $\tau = 700 \text{ ps}$ ). The decay times of the nonresonant (circles) QD's are relatively long in comparison to the resonant (squares)

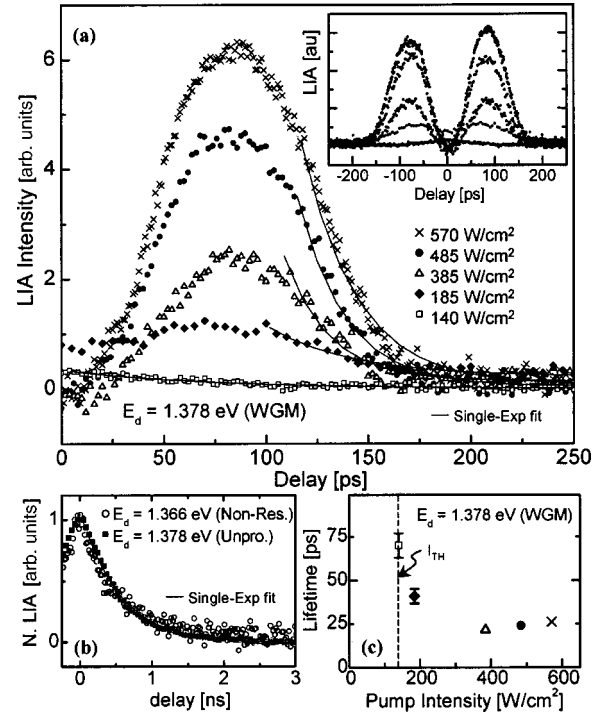


FIG. 4. (a) Intensity-dependent LIA data for QD's resonantly coupled to a WGM driven above lasing threshold ( $I_{TH} \sim 140 \text{ W cm}^{-2}$ ). Same LIA data plotted from  $-250$  to  $250 \text{ ps}$  (inset). (b) Normalized LIA data detected at QD emission nonresonant with the cavity, as well as ED QD's in the unprocessed region taken under high intensity ( $570$  and  $400 \text{ W cm}^{-2}$ , respectively), shows no dip at  $0$  delay. (c) Fitted lifetimes from right-most edge of data in (a) indicate a tripling of the resonant QD emission rate due to stimulated emission.

QD's, indicating that the significant reduction in lifetime is not due to enhanced nonradiative recombination from sample processing. Indeed, a sixfold shortening of the lifetime as compared to ED QD's outside the cavity reflects the modified vacuum field of the microdisk (Purcell effect),<sup>1</sup> revealing nonidealities in the coupling (note  $F_p \sim 50$ ). A summary of lifetimes extracted from LIA data taken under nonlasing conditions is shown in Fig. 3(b). The *filled* symbols are from QD's in unprocessed regions, while *unfilled* symbols are from QD's in the microdisk. Note that spontaneous emission lifetimes from resonant QD's can only be unambiguously extracted below their lasing thresholds. This will be addressed in the Fig. 4 discussion. Upon further review of Fig. 3(b), the intensity dependence from QD's that are nonresonant with the cavity (circles;  $E_d = 1.366 \text{ eV}$ ) is quite different than ED QD's outside the microdisk (filled circles). Near lasing threshold of a neighboring mode ( $E = 1.378 \text{ eV}$ ), nonresonant QD's *in the cavity* have longer lifetimes than ED QD's *outside the cavity*, indicating an inhibited spontaneous emission rate. However, above threshold, QD lifetimes *inside the cavity* begin to shorten. The transition at threshold may be due to the increased average number of photons in the cavity ( $N_p$ ) when lasing. Above threshold, emission rates should be further enhanced due to the increased number of photons in the cavity following the relation  $\Gamma_{TOT}$

$\approx \beta_{\text{sp}} F_P \Gamma_{\text{sp}} + v_g g_{\text{th}} N_P$ , assuming negligible nonradiative recombination where  $\Gamma_{\text{TOT}}$  is the total emission rate,  $\beta_{\text{sp}}$  is the spontaneous emission factor,  $\Gamma_{\text{sp}}$  is the intrinsic spontaneous emission rate,  $v_g$  is the group velocity of the mode of interest, and  $g_{\text{th}}[\text{cm}^{-1}]$  is the gain at threshold.<sup>16</sup>

We now focus on the coupling between resonant QD's and a high- $Q$  WGM at the onset of lasing. Figure 4(a) shows intensity-dependent LIA data for QD's detected at a WGM energy,  $E_d = 1.378$  eV. Clearly, the large dip at  $t=0$  delay in the LIA data is markedly different from the intensity dependence of QD's in the unprocessed material (Fig. 2). The 0 delay dip manifests in a shift of the peak position in the LIA signal from 0 to 86 ps, predominantly occurring at the lasing threshold. This nonmonotonic form of the LIA signal is not observed at similar pump intensities ( $>400$  W cm<sup>2</sup>) in non-resonant QD's within the microdisk (circles) or in ED QD's in unprocessed material (filled squares) [Fig. 4(b)], suggesting that the dip at 0 delay is associated with stimulated emission, a signature of *coherent* coupling between QD's and a WGM. Moreover, WGM's at  $E_d = 1.387$  and 1.396 eV in this microdisk, as well as other WGM's in other microdisks, show similar behavior at 0 delay above their lasing thresholds (not shown). The dip in the LIA signal may be due to a suppression of cross recombination due to the enhanced emission rate under stimulated emission.<sup>16</sup> However, further investigation into the mechanism is needed. We now fit the right-most edge of the LIA signal to a single exponential. Note that the fit is initiated at later times as the pump intensity is increased [shown in Fig. 4(a)]. Indeed, we observe a further enhancement (three times) in the resonant QD emission rate due to the increase in average photon density,  $N_P$ , by stimulated emission. The dip "half width" at 0 delay as

well as the saturation of the extracted lifetime ( $\tau \sim 25$  ps) at higher pump intensities may be limited by one or the combination of processes with comparable time scales: carrier capture time ( $\sim 20$  ps),<sup>5</sup> photon lifetime in the cavity ( $Q/\omega \sim 3$  ps), or stimulated emission lifetime.

Finally, we estimate the number of QD's coupling to the cavity. Given the QD density and diameter of the microdisks, we can estimate the total number of QD's in a microdisk ( $\sim 200$ ). Considering the  $Q$  of the cavity mode at lasing threshold ( $\sim 5000$ ) and neglecting the QD's lifetime dependence on emission energy, we can estimate the average number of QD's contributing to the WGM from the PL of the unprocessed region to be  $\sim 2$ . However, at pump intensities needed for lasing, homogeneous broadening ( $\sim 5$  meV) of a QD ground-state transition<sup>17</sup> may allow on average  $\sim 25$  QD's to weakly couple to a WGM due to partial spectral or spatial overlap. Using this value, the average photon number in this mode<sup>5</sup> is  $N_P \sim 1.9$ , indicating lasing action. Additionally, we find  $\beta_{\text{sp}} < 1$  ( $\sim 0.43$ ), consistent with an observed lasing threshold. In summary LIA spectroscopy is employed to study the *coherent* coupling between QD's and a high- $Q$  WGM in a single microdisk at the onset of lasing, revealing rich dynamics in the QD-cavity coupling and showing promise for studying ultrafast phenomena in solid-state systems for quantum information processing.

The authors would like to thank R. J. Epstein, J. A. Gupta, A. Imamoglu, and J. Levy for inspiring discussions. This work was supported by the AFOSR Grant No. F49620-02-1-0038; NSF Grant No. DMR-0071888, and DARPA/ONR Grant No. N00014-99-1-1096.

<sup>1</sup>E. M. Purcell, Phys. Rev. **69**, 681 (1946).

<sup>2</sup>Y. Yamamoto and R. E. Slusher, Phys. Today **46**, 66 (1993), and references therein; Y. Hanamaki, H. Akiyama, and Y. Shiraki, Semicond. Sci. Technol. **14**, 797 (1999); K. J. Luo *et al.*, Appl. Phys. Lett. **77**, 2304 (2000).

<sup>3</sup>P. Michler *et al.*, Science **290**, 2282 (2000); C. Santori *et al.*, Phys. Rev. Lett. **86**, 1502 (2001).

<sup>4</sup>J. M. Gerard *et al.*, Phys. Rev. Lett. **81**, 1110 (1998); G. S. Solomon, M. Pelton, and Y. Yamamoto, *ibid.* **86**, 3903 (2001).

<sup>5</sup>B. Gayral *et al.*, Appl. Phys. Lett. **78**, 2828 (2001); B. Gayral and J. M. Gerard, Physica E (Amsterdam) **7**, 641 (2000).

<sup>6</sup>A. Imamoglu *et al.*, Phys. Rev. Lett. **83**, 4204 (1999); R. J. Epstein *et al.*, Appl. Phys. Lett. **78**, 733 (2001).

<sup>7</sup>X. Fan, M. Lonergan, Y. Zhang, and H. Wang, Phys. Rev. B **64**, 115310 (2001).

<sup>8</sup>A. Olsson *et al.*, Appl. Phys. Lett. **41**, 659 (1982); Y. Yamada

*et al.*, Phys. Rev. B **52**, R2289 (1995); J. Levy *et al.*, Phys. Rev. Lett. **76**, 1948 (1996).

<sup>9</sup>B. Gayral *et al.*, Appl. Phys. Lett. **75**, 1908 (1999); P. Michler *et al.*, *ibid.* **77**, 184 (2000).

<sup>10</sup>S. L. McCall *et al.*, Appl. Phys. Lett. **60**, 289 (1992).

<sup>11</sup>The intensity of the pump beams is tuned to give equivalent PL contributions from each beam.

<sup>12</sup>R. Heitz *et al.*, Phys. Rev. B **56**, 10 435 (1997).

<sup>13</sup>E. Hanamura, Phys. Rev. B **37**, 1273 (1988).

<sup>14</sup>R. E. Slusher *et al.*, Appl. Phys. Lett. **63**, 1310 (1993).

<sup>15</sup>D. K. Young, Ph.D. thesis, University of California, Santa Barbara, 2002.

<sup>16</sup>L. A. Coldren and S. W. Corzine, *Diode Lasers and Photonic Integrated Circuits* (John Wiley, New York, 1995).

<sup>17</sup>T. Matsumoto, M. Ohtsu, K. Matsuda, T. Saiki, H. Saito, and K. Nishi, Appl. Phys. Lett. **75**, 3246 (1999).